Journal of Power Sources 185 (2008) 1225–1232

Contents lists available at ScienceDirect

Journal of Power Sources

journal homepage: www.elsevier.com/locate/jpowsour

Preparation and properties of carbon nanotube/polypropylene nanocomposite bipolar plates for polymer electrolyte membrane fuel cells

Shu-Hang Liao[a], Chuan-Yu Yen[a], Cheng-Chih Weng[a], Yu-Feng Lin[a], Chen-Chi M. Ma[a,*], Ching-Hung Yang[b], Ming-Chi Tsai[c], Ming-Yu Yen[a], Min-Chien Hsiao[a], Shuo-Jen Lee[d], Xiao-Feng Xie[e], Yi-Hsiu Hsiao[a]

[a] Department of Chemical Engineering, National Tsing Hua University, Hsin-Chu 30043, Taiwan, ROC
[b] Plastics Industry Development Center, Tai-Chung 40768, Taiwan, ROC
[c] Department of Engineering and System Science, National Tsing Hua University, Hsin-Chu 30043, Taiwan, ROC
[d] Fuel Cell Center, Yuan Ze University, Tao-Yuan 32003, Taiwan, ROC
[e] Institute of Nuclear and New Energy technology, Tsinghua University, Beijing 100084, PR China

ARTICLE INFO

Article history:
Received 14 May 2008
Received in revised form 10 June 2008
Accepted 11 June 2008
Available online 19 July 2008

Keywords:
Fuel cell
Bipolar plate
Nanocomposite
Carbon nanotubes
Graphite
Crystallinity

ABSTRACT

This study aims at the fabrication of lightweight and high performance nanocomposite bipolar plates for the application in polymer electrode membrane fuel cells (PEMFCs). The thin nanocomposite bipolar plates (the thickness <1.2 mm) consisting of multiwalled carbon nanotubes (MWCNTs), graphite powder and PP were fabricated by means of compression molding. Three types of polypropylene (PP) with different crystallinities including high crystallinity PP (HC-PP), medium crystallinity PP (MC-PP), low crystallinity PP (LC-PP) were prepared to investigate the influence of crystallinity on the dispersion of MWCNTs in PP matrix. The optimum composition of original composite bipolar plates was determined at 80 wt.% graphite content and 20 wt.% PP content based on the measurements of electrical and mechanical properties with various graphite contents. Results also indicate that MWCNTs was dispersed better in LC-PP than other PP owing to enough dispersed regions in nanocomposite bipolar plates. This good MWCNT dispersion of LC-PP would cause better bulk electrical conductivity, mechanical properties and thermal stability of MWCNTs/PP nanocomposite bipolar plates. In the MWCNTs/LC-PP system, the bulk electrical conductivities with various MWCNT contents all exceed 100 S cm^{-1}. The flexural strength of the MWCNTs/LC-PP nanocomposite bipolar plate with 8 phr of MWCNTs was approximately 37% higher than that of the original nanocomposite bipolar plate and the unnotched Izod impact strength of MWCNTs/LC-PP nanocomposite bipolar plates was also increased from 68.32 J m^{-1} (0 phr) to 81.40 J m^{-1} (8 phr), increasing 19%. In addition, the coefficient of thermal expansion of MWCNTs/LC-PP nanocomposite bipolar plate was decreased from 32.91 $\mu m\, m^{-1}\, ^{\circ}C^{-1}$ (0 phr) to 25.79 $\mu m\, m^{-1}\, ^{\circ}C^{-1}$ (8 phr) with the increasing of MWCNT content. The polarization curve of MWCNTs/LC-PP nanocomposite bipolar plate compared with graphite bipolar plate was also evaluated. These results confirm that the addition of MWCNTs in LC-PP leads to a significant improvement on the cell performance of the nanocomposite bipolar plate.

© 2008 Elsevier B.V. All rights reserved.

1. Introduction

In the recent years, the polymer electrolyte membrane fuel cell (PEMFC) has received intensive researches from both alternative energy and environmental consideration owing to their attractive features of high power density, low operating temperature and converting fuel to water as the only byproduct [1–4]. The key components of a fuel cell are the electrolyte, catalyst layer, gas diffusion layer and bipolar plates. Among these components, the bipolar plates provide the following main functions within the fuel cell stack [5]: provide a distribution of fuel gases within the cell, promote water management over the whole cell, separate the individual cells in the stack and carry electrical current away from membrane electrode assemblies (MEA). However, on the concept of commercial manufacturing for fuel cells, they are associated with major problems of high fabrication cost and insufficient reliability of fuel cells. Especially for bipolar plate (which accounts for nearly 38% in a fuel cell stack cost) [6], it is one of the most costly components in PEMFCs. Hence, the investigation on cost/performance materials of bipolar plates has become a critical research issue.

* Corresponding author. Tel.: +886 3571 3058; fax: +886 3571 5408.
E-mail address: ccma@che.nthu.edu.tw (C.-C.M. Ma).

0378-7753/$ – see front matter © 2008 Elsevier B.V. All rights reserved.
doi:10.1016/j.jpowsour.2008.06.097

To develop suitable materials for bipolar plates on the applications in fuel cells, the physical and electrical properties of bipolar plates should meet the following design requirements [7]:

- high electrical conductivity (>100 S cm^{-1})[1];
- low hydrogen permeability (<2 × 10^{-6} cm^3 (cm^2 s)$^{-1}$)[1];
- good chemical stability and corrosion resistant (<1 μA cm^{-2})[2];
- good flexural strength (>25 MPa)[1];
- high tensile strength (>41 MPa)[1];
- high thermal conductivity (>10 W (m K)$^{-1}$)[3];
- low thermal expansion;
- efficient processability.

The conventional materials for fabricating bipolar plate are based on either graphite materials or metals. The most commonly used bipolar plate material is graphite plates due to their advantages of high electrical conductivity, excellent corrosion resistance and lower density than those of metals. However, the disadvantages of graphite plates including the high cost resulted from machining channels into the surface and their brittleness would cause the fuel-cell stack to be heavy and voluminous [11,12]. Therefore, in the attempt to develop an alternative material, graphite-based polymer composite bipolar plates have been considered as the substitute for the conventional graphite plates. They exhibit lower cost, higher flexibility, lighter weight and easier manufacturing, the gas flow channels could be molded directly into the plate, eliminating the requirement for a costly machining step. However, the main problem of the polymer composite bipolar plate is the low electrical conductivity. Therefore, in the recent researches, graphite-based polymer composite bipolar plates have been fabricated from the combination of high concentration of graphites and additional conductive fillers to improve electrical conductivity [9–12]. The reinforced fillers used commonly including carbon nanotube, carbon fiber, and carbon black which have been incorporated into the composites to enhance overall performance of composite bipolar plates by conventional polymer processing technique [12,13]. However, several studies have also reported high electrical conductivity in composite bipolar plates at lower carbon loadings [14,15]. Blunk et al. [15] has developed epoxy/expanded graphite composite bipolar plates at 20 vol.% expanded graphite loadings that possess low area specific resistance (<20 mΩ cm^2) and also offer the opportunity to improve mechanical properties by incorporating other reinforced fillers.

In general, in order to fabricate composite bipolar plates in processing procedures, there are two different types of polymeric resins including thermoplastics and thermosets can be used. Comparing with these versatile polymer materials, polypropylene (PP) has the combination of the relatively low cost, good processability, well-balanced physical and mechanical properties [16,17]. It has been used to fabricate composite bipolar plates in the past few years [18]. Owing to the nonpolar functional groups in polypropylene backbone, it is difficult to improve the interfacial compatibility between additive filler and polymer matrix, and thus limit the improvement and usefulness of PP composite bipolar plates in fuel cells. However, in our previous study, Kuan et al. [19] indicated that a lower degree of crystallinity of polymer would provide a significant influence on the fillers–polymer interfacial adhesion, and provide a better dispersion of fillers within the polymer matrix. This phenomenon implies that introducing lower degree of crystallinity of polymer into the composite materials may be a possible method to further improve the properties of composite bipolar plates.

Additionally, among various reinforcements introduced into the polymer composites, carbon nanotubes (CNTs), which possess outstanding mechanical and electrical properties that have been applied to a great number of fields [20–22]. However, there are associated with two critical issues when CNTs were used as reinforcements in polymer composites [20–22]. First, CNTs tend to aggregate into ropes or bundles due to the strong intrinsic Van der Waals forces between them, and thus cause poor dispersion in polymer matrix. Moreover, smooth surface of CNTs and lack of interfacial bonding will result in weak interfacial adhesion between CNTs and matrix [23,24]. These two major problems would limit the improvement on the electrical or mechanical properties of composites by CNTs. A common approach reported so far is the surface modifications or functionalizations of CNTs [23–28]. However, this process may damage the molecular framework of CNTs, such as breaking their sidewall and turning into amorphous carbon, reduce the mechanical properties and decrease the electrical conductivity of composites [25–28]. Several literatures have indicated that the physical method related to melt blending is one of the most promising routes [29–31]. When composite materials were prepared by melt blending, the high shear force leads to better interactions between CNTs and polymer matrix without damaging the structure of CNTs, resulting in good processability and better performance of the composites [32]. Hence, melt blending method would be considered as an effective method to enhance the dispersion of CNTs in polymer.

In this study, MWCNTs/PP nanocomposite bipolar plates for use in fuel cells were developed by melt blending process. Three different degrees of crystallinity of PP were introduced into MWCNTs/PP nanocomposite bipolar plates to investigate the interfacial compatibility between PP and MWCNTs. Furthermore, the electrical conductivity and mechanical property of MWCNTs/PP nanocomposite bipolar plates were measured to optimize the graphite content. The effects of MWCNTs incorporated with three types of PP on electrical, mechanical, thermal properties as well as their single cell performance of nanocomposite bipolar plates were also investigated.

2. Experimental

2.1. Materials

Three types of commercial grade polypropylene (PP, were assigned as 1120, 4204 and 3354 with melt flow indices (MFI) of 1.7, 1.9 and 3.5 g/10 min) used as the polymer matrix which were supplied from the Yung Chia Chemical Ind., Co., Ltd., Taiwan. MWCNTs were received from the CNT Co., Ltd., Korea (MWCNT, trade name: $C_{tube\ 100}$; purity: 95%) with the length of 1–25 μm and average 10–50 nm in diameter. Graphite powder was provided by the Great Carbon Co. Ltd., Taiwan, which has a density of 1.88 g cm^{-3} and the particle size is less than 1000 μm.

2.2. Preparation of MWCNTs nanocomposite bipolar plates

2.2.1. Melt compounding and compression molding

PP, MWCNTs and graphite powders were melt-mixed by means of a Brabender, and then the molten compounds were obtained in the mixer. The mixing time was set at 180 °C for 10 min, and the rotational speed was 50 rpm. Then, the molten compounds were pulverized to form a powder. The powder was compression molded by a hydraulic press at a pressure of 70 kg cm^{-2} and 170 °C for 15 min.

[1] DOE (Department of Energy, USA) targets for bipolar plates [8].
[2] Corrosion resistance target of Corrosion Science [10].
[3] Targets of Plug Power Co. for bipolar plates [9].

2.2.2. Characterization of MWCNTs/PP nanocomposite bipolar plates

Thermal analysis measurements were performed utilizing a differential scanning calorimeter (PYRIS Diamond DSC, Perkin Elmer Co., USA). Five milligrams sample was heated from 30 °C to 200 °C at a scan rate of 10 °C min^{-1} and maintained at that temperature for 10 min to eliminate any previous thermal history of the material. Subsequently, the sample was cooled to 30 °C at a scan rate of 50 °C min^{-1}. Three types of PP with low, medium and high degree of crystallinities were denoted hereafter as LC-PP, MC-PP and HC-PP, respectively, in this study. The microstructure of MWCNTs/PP nanocomposites was observed using a Scanning Electron Microscope (SEM, JSM 840A, JEOL Co., Tokyo). The electrical resistivity of composite bipolar plate was detected using a four-point probe detector (C4S-54/5S, Cascade Microtech, Beaverton, OR, USA). The flexural strength of composite bipolar plates with the dimensions of 60.0 mm × 13.0 mm × 3.0 mm ($L \times W \times T$) was measured by an Instron Model 4468 universal tester according to ASTM D-790 method. The unnotched Izod impact tests were performed on a Tinius Olsen 92T Impact Tester based on ASTM D-256. The sample dimensions were 64.0 mm × 12.7 mm × 3.3 mm. The coefficient of thermal expansion (CTE) was measured by a Themomechanical Analyzer (TMA2940, DuPont, USA) at a temperature range from 30 °C to 145 °C in both the *X* and *Y* direction according to ASTM D-696 [33].

2.2.3. Single fuel cell stack integration and performance tests

A single stack PEMFC cell test was developed at our laboratory as reported in our previous papers [12,27]. The catalyst ink for the electrodes was prepared by mixing the catalyst powder (20 wt.% Pt/C, E-TEK), Nafion® solution, and *iso*-propyl alcohol. The catalyst ink was coated onto the wet-proof carbon paper so that the catalyst layer with a platinum loading of 0.4 mg cm^{-2} was prepared. The anode and cathode were prepared with the same amount of loadings. Then the electrodes at both sides were hot-pressed onto the pre-treated Nafion®115 membrane to fabricate the membrane-electrode assembly (MEA) at 140 °C and 200 kg cm^{-2} for 90 s. The active electrode area was 4 cm^2.

A single fuel cell was constructed from the prepared MEA, Teflon gasket, and the prepared nanocomposite bipolar plate on both sides of the MEA. The thickness of the nanocomposite bipolar plate was 1.2 mm. The single fuel cell was operated at 60 °C and 1 atm. Hydrogen and oxygen gases which acted as the fuel and the oxidant were fed to the anode and cathode, respectively. The flow rate of both gases was kept at 1/1 L min^{-1}. The performance of the single fuel cell was evaluated by measuring the *I–V* characteristics using an electronic load facility (Agilent, N3301A).

3. Results and discussion

3.1. Effect of graphite contents on the properties of the composite bipolar plates

In order to study the effects of graphite contents on the properties of composite bipolar plates, the effect of graphite content on the bulk electrical conductivity of MC-PP composite bipolar plates was investigated. Fig. 1 presented that the bulk electrical conductivity increases with the increasing of graphite content. When graphite loading was exceeded 77.5 wt.%, the bulk electrical conductivity would exceed 100 S cm^{-1} (which can meet the bulk electrical conductivity requirement of DOE for composite bipolar plates [9]). Several studies have indicated that the electrical conductivity of the composites depends on mutual contact of the conductive materials to further generate conductive paths throughout the composites

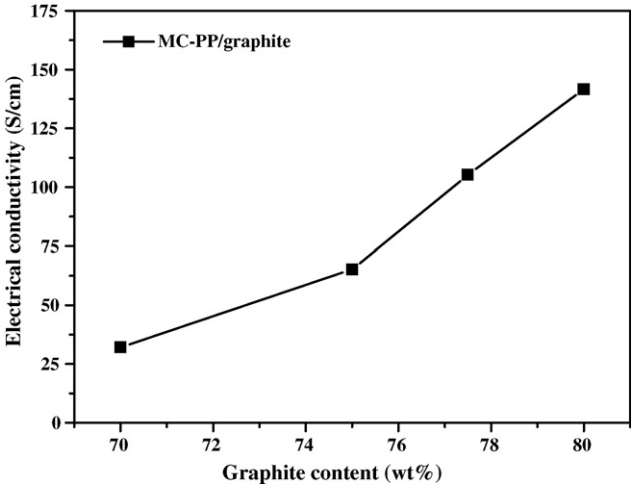

Fig. 1. Effect of graphite contents on the bulk electrical conductivities of the composite bipolar plates.

[15,34,35]. In this case, by decreasing the content of insulating PP matrix, the number and magnitude of conductive graphites will be increased, and thus will establish more electrical conductive paths to provide current carrier flow in the composite bipolar plate.

Additionally, the composite bipolar plates not only require high electrical conductivity but also should need sufficient mechanical strength to support every component in the fuel-cell stack and withstand sudden impact or shaking [15,27]. Therefore, the flexural and impact properties of the MC-PP composite bipolar plates were also investigated by adding various graphite contents. It could be seen from Fig. 2 that the flexural strength of the MC-PP composite bipolar plates was increased with the increasing of graphite content. When the graphite content was reached 80 wt.%, the maximum flexural strength of the composite bipolar plates was measured at 23.66 MPa. These results were attributed to the fact that the graphite powder possesses stiffer and rigid properties than that of PP [36,37]. Therefore, the flexural strength of composite bipolar plates will be enhanced with the increasing of graphite content. However, the flexural strength was still below DOE target value (>25 MPa). This result was mainly due to the fact that during the fabricating of the composite bipolar plates, the pulverized-process

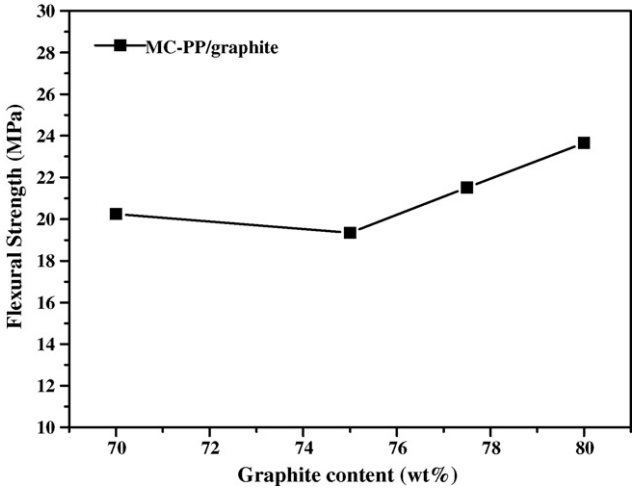

Fig. 2. Effect of graphite contents on the flexural strengths of the composite bipolar plates.

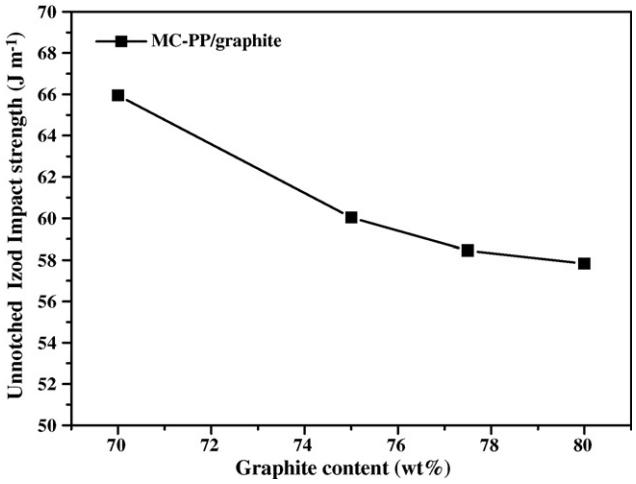

Fig. 3. Effect of graphite contents on the unnotched Izod impact strengths of the composite bipolar plates.

may smash the composites to form powdered that will reduce their mechanical properties drastically.

Fig. 3 shows the effect of graphite content on the unnotched Izod impact strength of these composite bipolar plates. The unnotched Izod impact strength was decreased from 66.73 J m^{-1} to 58.66 J m^{-1}, as the graphite content was increased to the range of 70–80 wt.%. Since PP possesses outstanding impact resistance than graphite, hence, a decreased tendency of the unnotched Izod impact strength at high graphite loading was observed. The unnotched Izod impact strengths of the composite bipolar plates with various graphite contents (from 70 to 80 wt.%) all still exceed the target value of Plug Power Co. (>40.5 J m^{-1}).

Based on the investigations of electrical and mechanical properties discussed above, it was found that the optimum composition would be considered at 80 wt.% graphite content and 20 wt.% PP loading for composite bipolar plates and the maximum values of the bulk electrical conductivity (>100 S cm^{-1}), the flexural strength (23.66 MPa), and the unnotched Izod impact strength were obtained for composite bipolar plates (58.66 J m^{-1}). Furthermore, owing to their low flexural strength, CNTs were introduced into the composite bipolar plates to improve the flexural property.

Table 1
Thermal properties and crystallinity of MWCNTs/PP nanocomposites with 4 phr[a] of MWCNTs

Type of nanocomposite bipolar plate	T_c (°C)	ΔH_c (J g^{-1})	X_c (%)	Ethylene content[b] (%)
MWCNTs/HC-PP/graphite	140.5	18.7	45.1	0
MWCNTs/MC-PP/graphite	135.9	15.8	38.1	5–7
MWCNTs/LC-PP/graphite	134.7	14.5	35.0	14

[a] phr: parts per hundred parts of PP resin.
[b] Date were obtained from Yung Chia Chemical Company.

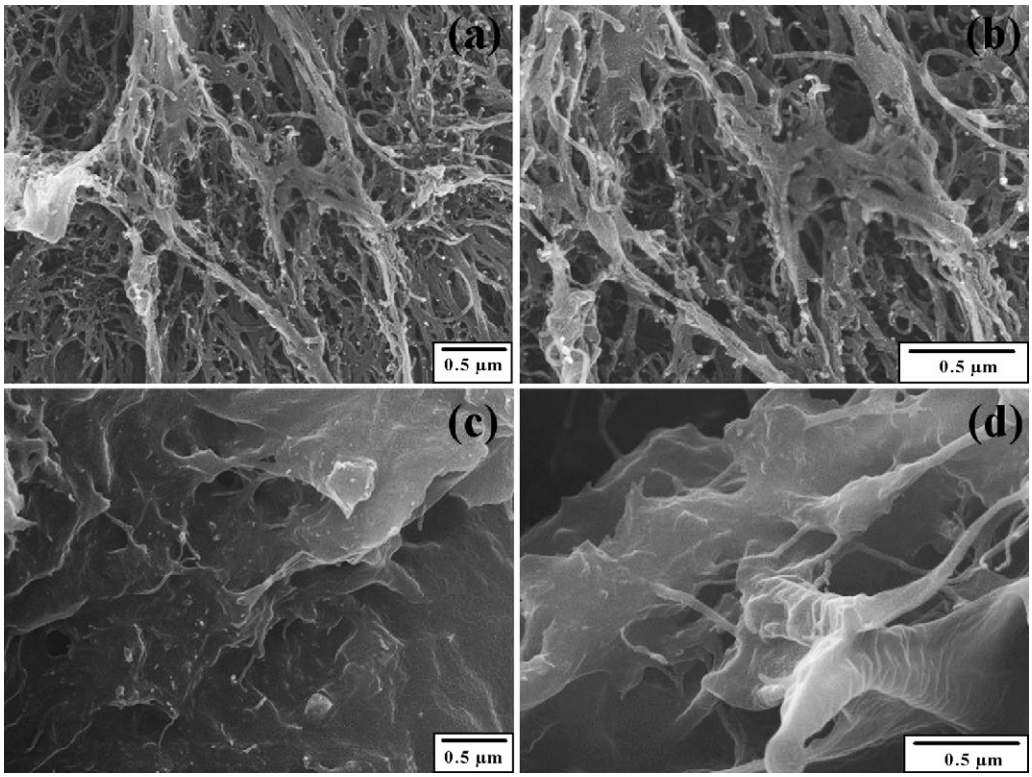

Fig. 4. SEM photographs of carbon nanotubes on the fracture surface of different PP matrices: MWCNTs/HC-PP (a) × 30,000, cross section (b) × 50,000, cross section; MWCNTs/LC-PP (c) × 30,000, cross section (d) × 50,000, cross section.

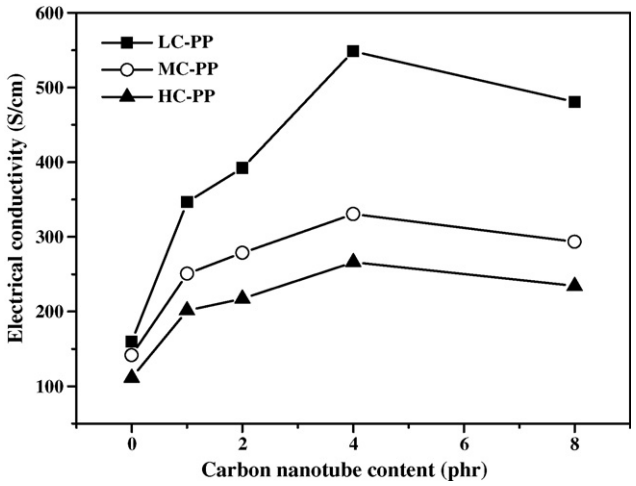

Fig. 5. The bulk electrical conductivities of the nanocomposite bipolar plates with-various MWCNT contents.

3.2. *Effect of PP crystallinity on the dispersion of MWCNTs in the nanocomposite bipolar plates*

Several reports have indicated that the crystalline characteristics of polymers including crystallinity, spherulite size and structure will provide significant effects on physical properties of thermoplastics or their composites [38–40]. In this study, the ethylene–propylene copolymer (EPC) used was formed by the copolymeriztion of ethylene and propylene. The different compositions of ethylene and propylene group would cause a variety of heterogeneous phases formed in PP resin, and reflect directly on the different degrees of crystallinity.

Therefore, in order to investigate the degree of crystallinity of MWCNTs/PP nanocomposite bipolar plates, the thermal properties including the crystallization temperature (T_c), the crystallization heat (ΔH_c) and the degree of crystallinity (X_c) were conducted by DSC. The crystallinity of MWCNTs/PP nanocomposite bipolar plates was evaluated based on the following equation [38]:

$$X_c\ (\%) = \frac{\Delta H_c}{\Delta H_c^{\circ} \times W_{polymer}} \quad (1)$$

where ΔH_c is the specific melting heat of sample, ΔH_c° is the theoretical specific melting heat of 100% crystallinity of PP (209 J g^{-1}) [38], and $W_{polymer}$ is related to the weight fraction of PP in the nanocomposite bipolar plates. In MWCNTs/PP nanocomposite bipolar plates, it was obvious that ΔH_c and X_c were decreased gradually with the increasing of ethylene content, where X_c related to ethylene contents were 35.0% (14 wt.%), 38.1% (5–7 wt.%) and 45.1% (0 wt.%), respectively, as shown in Table 1. These results indicate that the more heterogeneous phase resulted from ethylene in PP may hinder the folding chain of PP molecular chain during crystal formation, and thus cause further decrease of crystalline regions of MWCNTs/PP nanocomposite bipolar plates [41].

Additionally, the microphotographs of the fractured surfaces of the MWCNTs/PP nanocomposites were performed to study the dispersion of MWCNTs in the nanocomposite materials, as exhibited in Fig. 4. It can be seen that HC-PP matrix loaded with MWCNTs shows non-uniform dispersion and MWCNTs tend to aggregate into larger clusters due to their strong intertublar Van deer Waals force. Meanwhile, numerous MWCNTs were pulled out from the HC-PP matrix, as can be observed from Fig. 4a and b. This phenomenon was resulted from poor compatibility between MWCNTs and PP matrix. In contrast to MWCNTs/HC-PP, the presence of MWCNTs in LC-PP matrix showed better and homogeneous dispersion, as shown in Fig. 4c and d. Almost no large quantity of MWCNTs was aggregated, and MWCNTs were coated by PP matrix and adhered tightly. In our previous study, Kuan et al. [19] has indicated that most of the MWCNTs were dispersed mainly in the non-crystalline region but absent in the crystalline region of the polymer. Xia et al. [42] has also reported that the low crystallinity polymer system could coat the conducting materials such as graphite particles more uniformly.

Considering the lower degree of crystallinity of MWCNTs/LC-PP nanocomposites, they have much more non-crystalline regions which may promote the dispersion of MWCNTs uniformly without aggregation, consequently, leading to a better dispersion of MWCNTs in LC-PP matrix than in HC-PP matrix. The interfacial adhesion between filler and polymer matrix will be enhanced by the better MWCNT dispersion in the lower crystalline polymer matrix. As a result, the relative compatibility between filler and polymer matrix was in the order of MWCNTs/LC-PP > MWCNTs/MC-PP > MWCNTs/HC-PP.

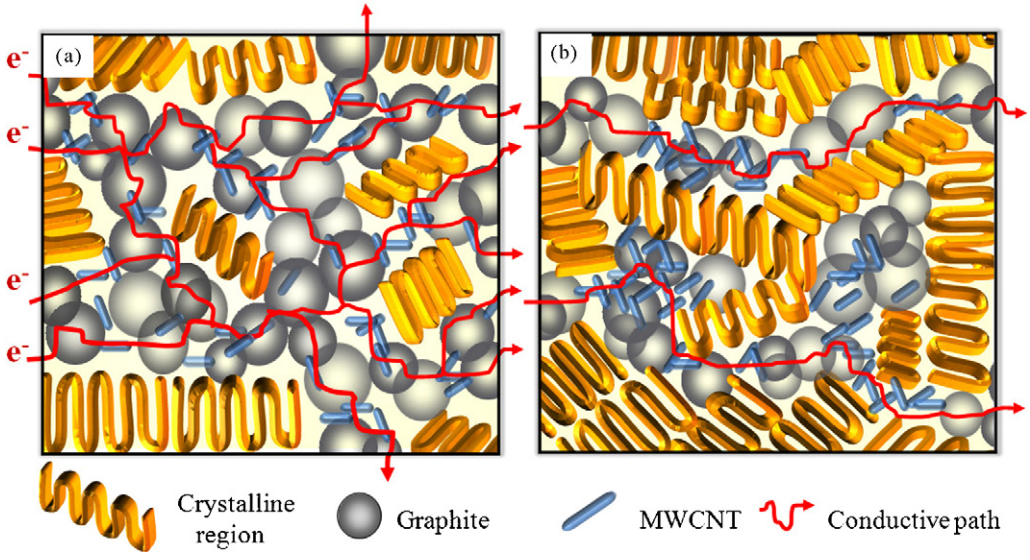

Fig. 6. The model of conductive paths in the nanocomposite bipolar plates with (a) better dispersion of MWCNTs in LC-PP matrix (b) MWCNTs aggregation in HC-PP matrix.

3.3. Bulk electrical conductivity of the nanocomposite bipolar plates containing MWCNTs

A number of reports have indicated that the incorporation of graphite with other conductive materials, especially carbon nanotubes, has been considered as an effective method to develop higher bulk electrical conductivity of the nanocomposite bipolar plates due to 3D conductive networks [20–22]. Therefore, the bulk electrical conductivity of nanocomposite bipolar plates with various MWCNT contents was measured, as shown in Fig. 5. Three types of MWCNTs/PP nanocomposite bipolar plates all have promising bulk electrical conductivity, above the DOE target value of 100 S cm^{-1}. Results also show that the bulk electrical conductivities of the nanocomposite bipolar plates was increased dramatically with the increasing of MWCNT content and then decreased slightly with higher MWCNT loading. Since, the incorporation of a small quantity of MWCNTs into polymer composites could exhibit higher electrical conductivity due to the formation of extra effective electrical conducting paths [27]. However, higher MWCNT loading in polymer composites may cause serious MWCNT aggregation, and the bulk electrical conductivity will be leveled off, even decreased.

Additionally, the bulk electrical conductivity was increased significantly in the order of MWCNTs/LC-PP > MWCNTs/MC-PP > MWCNTs/HC-PP nanocomposite bipolar plates. For instance, at 4 phr MWCNT content, the bulk electrical conductivities of MWCNTs/LC-PP, MWCNTs/MC-PP and MWCNTs/HC-PP nanocomposite bipolar plates were measured at 548, 330 and 266 S cm^{-1}, respectively. Similar trend was also observed that the bulk electrical conductivity increased as the degree of crystallinity of MWCNTs/PP nanocomposite bipolar plates reduced at the same MWCNT loading. Based on these reports mentioned above [19,42] and the SEM microphotographs, this phenomenon may be attributed to the better dispersion of MWCNTs in LC-PP matrix than other PP matrices [19]. The probability of self-aggregation in the conductive materials will be reduced, and thus, more electrical conducting paths were built up by the binary conductive materials system (which is assumed to consist of MWCNTs and graphites throughout the nanocomposite bipolar plates) [18]. Consequently, the nanocomposite bipolar plates containing lower crystallinity of PP could exhibit higher bulk electrical conductivity.

Fig. 6 depicts a proposed model of conductive paths in the MWCNTs/PP nanocomposite bipolar plate with different crystallinities of PP matrices. This model was based on the presented experimental results. Electrical insulated polymers are filled with electrically conductive graphites and carbon nanotubes. The insulting zones between graphites are bridged by the MWCNTs. When voltage is applied, more continuous paths are available for the flow of electrical current due to the MWCNT homogeneity in LC-PP matrix. Comparing these two conductive-path models, it is assumed that more electrical conductive paths were formed effectively by the better dispersed MWCNTs and graphite particles in LC-PP than that of HC-PP.

3.4. Effect of MWCNT contents on mechanical properties of the nanocomposite bipolar plates

In addition to high bulk electrical conductivity, the high performance bipolar plates should also provide the required mechanical strength to be used in the fuel-cell stacks. However, it is difficult to develop the composite plates with the combination of high conductivity and high enough mechanical properties [43,44]. This issue has become the critical goal attracted a great number of attentions. As shown in Fig. 7, the flexural strengths of the nanocomposite bipolar plates were increased with the increasing of MWCNT content. As MWCNT content was at 8 phr, the flexural strengths of MWCNTs/LC-PP, MWCNTs/MC-PP, and MWCNTs/HC-PP nanocomposite bipolar plates were increased from 21.43, 23.73 and 25.91 MPa (0 phr) to 29.46, 31.71 and 33.62 MPa (8 phr), respectively.

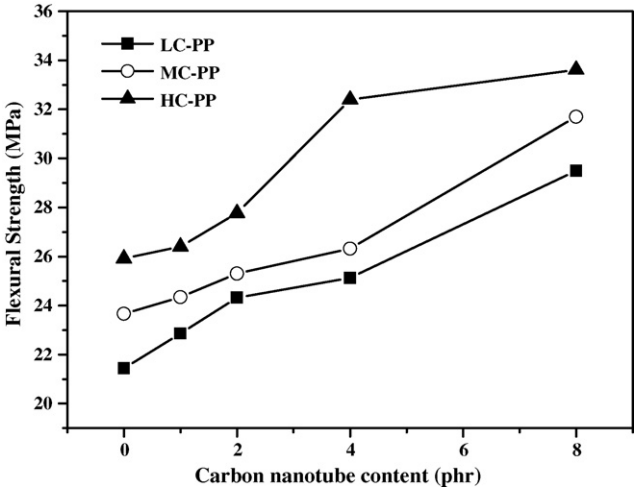

Fig. 7. The flexural strengths of the nanocomposite bipolar plates with various MWCNT contents.

These results reveal that the existence of MWCNTs in the nanocomposite bipolar plates can be considered as stress concentrators. Owing to their rigidity and high-aspect ratio, the load transfered toward the MWCNTs [27,45] will improve effectively the stiffness of the nanocomposite bipolar plates. Although the low crystallinity of LC-PP possesses looser structure, the flexural strengths of MWCNTs/LC-PP nanocomposite bipolar plates were lower than these of MWCNTs/LC-PP and MWCNTs/HC-PP systems. However, the improvement of the flexural strength was increased apparently in the order of MWCNTs/LC-PP (37%) > MWCNTs/MC-PP (34%) > MWCNTs/HC-PP (30%). Since the better interfacial compatibility between MWCNTs and LC-PP matrix will promote the formation of a filler-polymer network structures, and thus enables the nanocomposite bipolar plate to transfer the load from the polymer matrix to MWCNTs more efficiently. Hence, the MWCNTs/LC-PP nanocomposite bipolar plates with the better compatibility between fillers and polymer resin have the greater reinforcement of the flexural strength.

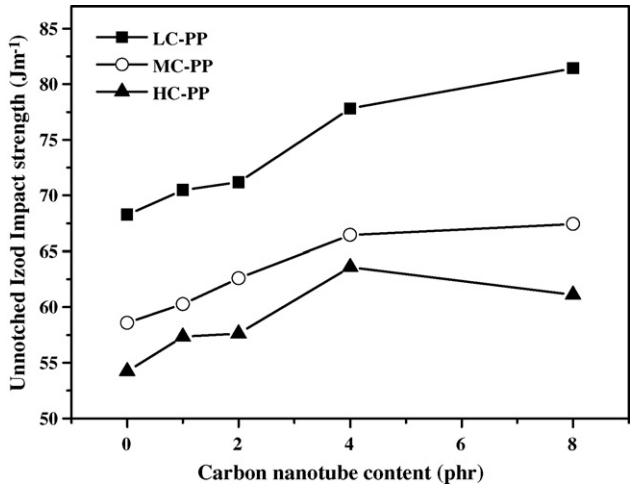

Fig. 8. The unnotched Izod impact strengths of the nanocomposite bipolar plates with various MWCNT contents.

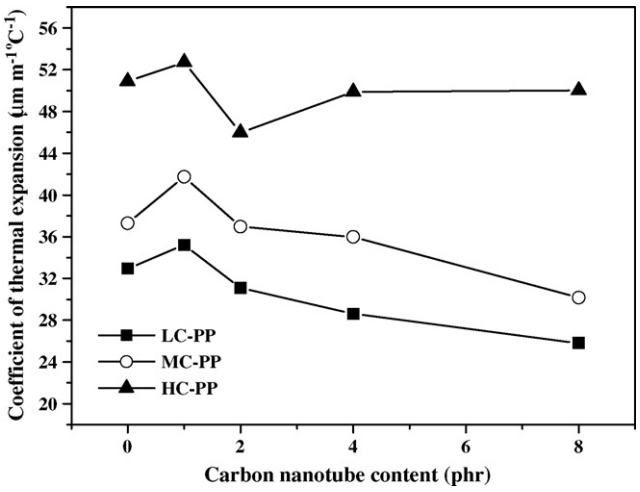

Fig. 9. The coefficients of thermal expansion of the nanocomposite bipolar plates with various MWCNT contents.

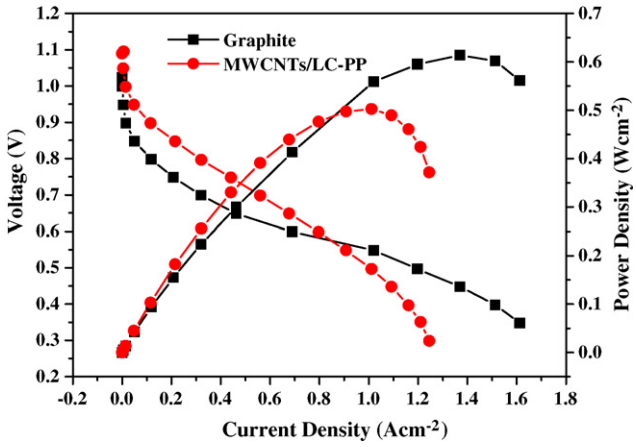

Fig. 10. The I-V and I-P curves of the LC-PP nanocomposite bipolar plate (with 80 wt.% graphite and 4 phr of MWCNTs) and graphite bipolar plate.

The unnotched Izod impact strength of nanocomposite bipolar plates was also investigated, as shown in Fig. 8. The unnotched Izod impact strengths of nanocomposite bipolar plates with the increasing of MWCNT content were similar to the trend of the flexural strength. As 8 phr of MWCNTs was incorporated into LC-PP, MC-PP and HC-PP nanocomposite bipolar plates, the impact strengths were increased to 81.40, 67.42 and 61.13 J m^{-1}, respectively. In this case, the impact strength of MWCNTs/LC-PP nanocomposite bipolar plates was much higher than these of MWCNTs/MC-PP and MWCNTs/HC-PP nanocomposite bipolar plates. Generally, the copolymerization of ethylene and propylene, acting as a more effective method to improve the impact strength of PP resin [46,47]. In this study, LC-PP polymer used herein contains a higher copolymer ratio (14 wt.%) than that of MC-PP (5–7 wt.%) and HC-PP (0 wt.%) polymer resin, and thus the MWCNTs/LC-PP nanocomposite bipolar plates will exhibit higher toughness apparently.

Moreover, the enhancement of the unnotched Izod impact strength for the nanocomposite bipolar plates was increased in the order of MWCNTs/LC-PP > MWCNTs/MC-PP > MWCNTs/HC-PP. From these results, it was postulated that better dispersion and good compatibility between MWCNTs and LC-PP matrix will induce stronger adhesion between MWCNTs and LC-PP matrix without aggregation. Therefore, it was found that the impact strengths of MWCNTs/LC-PP nanocomposite bipolar plates were improved effectively similar to the trend of the flexural strengths.

From the above evidence, all of the MWCNTs/PP nanocomposite bipolar plates developed in this study possess the promising mechanical property when the MWCNT loading exceeds 4 phr, exceeding DOE and Plug Power Co. target value (the flexural strength > 25 MPa and the impact strength > 40.5 J m^{-1}, respectively).

3.5. *Effect of MWCNT contents on the thermal expansion behaviors of the nanocomposite bipolar plates*

Thermal mechanical analysis was carried out to investigate the thermal stability of nanocomposite bipolar plates. As shown in Fig. 9, the coefficient of thermal expansion (CTE) decreased with the increasing of MWCNT content in the range 1–8 phr loading. The CTE of nanocomposite bipolar plates with 8 phr of MWCNTs incorporated with LC-PP, MC-PP and HC-PP resin were decreased from 32.91, 37.32 and 50.90 (0 phr of MWCNTs) to 25.79, 30.21 and 50.12 μm mm^{-1} °C^{-1}, respectively. Since MWCNTs possess much better thermal stability than that of PP at elevated temperature, as expected, leading to the decrease in CTE as MWCNT content increased [27]. However, results demonstrated an increase in CTE as 1 phr of MWCNTs was incorporated into MWCNTs/PP nanocomposite bipolar plates. It was suggested that the lower content of MWCNTs may cause the de-entanglement of polymer chains resulted in an increase of the free volume of nanocomposite bipolar plates corresponding to an increase of CTE.

Moreover, it was also noteworthy to notice that HC-PP system showed higher thermal expansion behavior among all of the nanocomposite bipolar plates. For the compact structural material such as polymer with high crystallinity, polymer chains not only move or extend difficulty but also may be expanded outward resulted from fewer spaces within the nanocomposite bipolar plates. By contrary, the loose materials such as lower crystallinity of polymer could provide more spaces to decrease the effects of the thermal expansions [2]. Therefore, a lower thermal expansion behavior of MWCNTs/LC-PP nanocomposite bipolar plates occurred at elevated temperature.

Furthermore, for MWCNTs/LC-PP nanocomposite bipolar plates, the effect of MWCNTs on the thermal expansion was decreased apparently. The reasonable interpretation may be due to better dispersion of MWCNTs in LC-PP polymer matrix, resulting in the greater enhancement of thermal stability of nanocomposite bipolar plates. On the contrary, as the MWCNT loading was above 4 phr, the

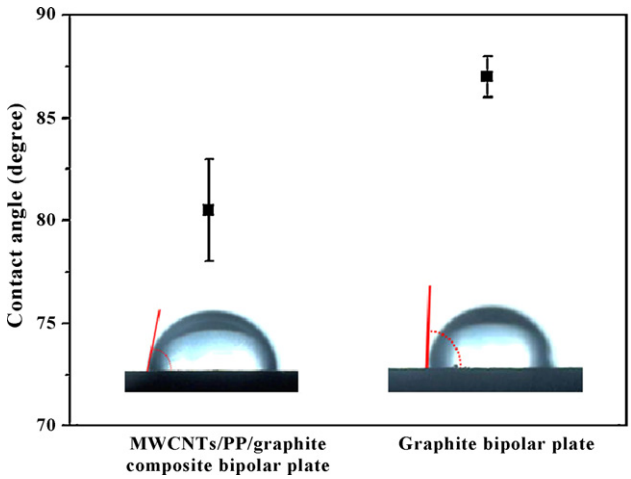

Fig. 11. The contact angles of the LC-PP nanocomposite bipolar plate (with 80 wt.% graphite and 4 phr of MWCNTs) and graphite bipolar plate.

CTE of MWCNTs/HC-PP nanocomposite bipolar plate was increased mainly due to the aggregation of MWCNTs. Based on these results, it is clear indicated that the enhancement of the compatibility between MWCNTs and PP will cause better thermal stability of the nanocomposite bipolar plates.

3.6. Single cell performance test

This study also evaluates the *I–V* and *I–P* performances of a nanocomposite bipolar plate (with the composition containing 80 wt.% graphite, 20 wt.% LC-PP and 4 phr of MWCNTs) and graphite bipolar plate. The *I–V* and *I–P* curves of the single cell using the nanocomposite bipolar plates were presented in Fig. 10. First, over the median current density region, the possibly improved performance could be observed. It is postulated that the flexibility of MWCNTs/LC-PP nanocomposite bipolar plates could effectively help to reduce the interfacial contact resistance between the MEA and bipolar plates during the compressively assembling a single cell. Therefore, the single cell using MWCNTs/LC-PP nanocomposite bipolar plates exhibited lower ohmic resistance than using graphite bipolar plates, and thus leading to higher performance.

Furthermore, at the mass transfer controlled region (high current density), the result reflected that MWCNTs/LC-PP nanocomposite bipolar plates with relatively small contact angle (approaching 80.5°) may lead to difficult water transfer. Contrarily, the hydrophobic graphite bipolar plates with higher water contact angle (approaching 87°) could help to repel water from the cathode [48] and will exhibit higher current density, as shown in Fig. 11. Consequently, the present system of MWCNTs/LC-PP nanocomposite bipolar plate has the maximum current density and power density, 1.245 and 0.503 W cm^{-2}, respectively. Furthermore, the maximum power density of MWCNTs/LC-PP nanocomposite bipolar plates only slightly lower than that of graphite bipolar plate corresponding to 0.614 W cm^{-2} comparatively.

4. Conclusions

In this study, a novel polymer nanocomposite bipolar plate composed of MWCNTs, PP and graphite powder has been prepared successfully by melt blending and compression molding. The optimum composition of composite bipolar plate was evaluated at 20 wt.% PP and 80 wt.% graphite based on electrical and mechanical properties. Furthermore, results also reveal that three types of nanocomposite bipolar plates incorporated with MWCNTs could improve bulk electrical conductivity, flexural strength, unnotched Izod impact strength and thermal expansion properties (meeting the requirements of DOE or industrial targets). Especially for LC-PP system, the dispersion of MWCNTs in nanocomposite bipolar plates was enhanced very effectively, consistent with the microphotographs by SEM. This reason is mainly resulted from enough dispersible regions for MWCNTs, and thus the improvement of MWCNTs in LC-PP nanocomposite bipolar plates was much higher than that of MC-PP and HC-PP systems. In the *I–V* and *I–P* performance tests, the maximum current density and power density were measured at 1.245 A cm^{-2} and 0.503 W cm^{-2}, respectively, for the optimum composition of nanocomposite bipolar plate (4 phr of MWCNTs, 20 wt.% LC-PP and 80 wt.% graphite). This observation indicates that these nanocomposite bipolar plates with the high cell performance may have great potential for the application in fuel cells.

Acknowledgements

The authors were grateful to the Plastic Industry Development Center (PIDC), Taiwan, for assistance with the instrumentations. Financial support by Fuel Cell Center of Yuan-Ze University, Taiwan, is also great appreciated.

References

[1] B.C.H. Steele, A. Heinzel, Nature 414 (2001) 345.
[2] H.C. Kuan, C.C.M. Ma, K.H. Chen, S.M. Chen, J. Power Sources 134 (2004) 7.
[3] A. Hermann, Int. J. Hydrogen Energy 30 (2005) 1297.
[4] A. Muller, P. Kauranen, A.V. Ganski, B. Hell, J. Power Sources 154 (2006) 467.
[5] L. Du, S.C. Jana, J. Power Sources 172 (2007) 734.
[6] S.R. Dhakate, R.B. Mathur, B.K. Kakati, T.L. Dhami, Int. J. Hydrogen Energy 32 (2007) 4537.
[7] B.D. Cunningham, J. Huang, D.G. Baird, J. Power Sources 165 (2007) 764.
[8] K. RoBberg, V. Trapp, Handbook of Fuel Cells—Fundamentals, Technology and Applications, John Wiley & Sons, Ltd., New York, 2003, pp. 308–314.
[9] J.K. Kuo, C.K. Chen, J. Power Sources 162 (2006) 207.
[10] I.E. Paulauskas, M.P. Brady, H.M. Meyer III, R.A. Buchanan, L.R. Walker, Corros. Sci. 48 (2006) 3157.
[11] B.D. Cunningham, D.G. Baird, J. Power Sources 168 (2007) 418.
[12] C.Y. Yen, S.H. Liao, Y.F. Lin, C.H. Hung, Y.Y. Lin, C.C.M. Ma, J. Power Sources 162 (2006) 309.
[13] J. Scholta, B. Rohland, V. Trapp, U. Focken, J. Power Sources 84 (1999) 231.
[14] H. Wolf, M.W. Porada, J. Power Sources 153 (2006) 41.
[15] R. Blunk, M.H.A. Elhamid, D. Lisi, Y. Mikhail, J. Power Sources 156 (2006) 151.
[16] M.A. Lo'pez Manchado, L. Valentini, J. Biagiotti, J.M. Kenny, Carbon 43 (2005) 1499.
[17] C.D. Rosa, F. Auriemma, O.R. de Ballesteros, L. Resconi, I. Camurati, Chem. Mater. 19 (2007) 5122.
[18] R. Dweiri, J. Sahari, J. Power Sources 171 (2007) 424.
[19] C.F. Kuan, H.C. Kuan, C.C.M. Ma, J. Phys. Chem. Solids 69 (2008) 1395.
[20] S. Iijima, Nature 345 (1991) 56.
[21] D.M. Delozier, K.A. Watson, J.G. Smith Jr., T.C. Clancy, J.W. Connell, Macromolecules 39 (2006) 1731.
[22] Y. Yang, X. Xie, J. Wu, Z. Yang, X. Wang, Y.W. Mai, Macromol. Rapid Commun. 27 (2006) 1695.
[23] H.J. Lee, S.J. Oh, J.Y. Choi, J.W. Kim, J. Han, L.S. Tan, J.B. Back, Chem. Mater. 17 (2005) 5057.
[24] S. Li, Y. Qin, J. Shi, Z.X. Guo, Y.F. Li, D. Zhu, Chem. Mater. 17 (2005) 130.
[25] A. Star, J.F. Stoddart, D. Steuerman, M. Diehl, A. Boukai, E.W. Wong, X. Yang, S.W. Chung, H. Choi, J.R. Health, Angew. Chem., Int. Ed. 40 (2001) 1721.
[26] J. Sun, L. Gao, Carbon 41 (2003) 1063.
[27] S.H. Liao, C.H. Hung, C.C.M. Ma, C.Y. Yen, Y.F. Lin, C.C. Weng, J. Power Sources 176 (2008) 175.
[28] C.H. Tseng, C.C. Wang, C.Y. Chen, Chem. Mater. 19 (2007) 308.
[29] M.K. Seo, S.J. Park, Chem. Phys. Lett. 395 (2004) 44.
[30] I. Alig, D. Lellinger, S.M. Dudkin, P. Potschke, Polymer 48 (2007) 1020.
[31] P. Potschke, A.R. Bhattacharyy, A. Janke, Carbon 42 (2004) 965.
[32] Z. Zhang, J. Zhang, P. Chen, B. Zhang, J. He, G.H. Hua, Carbon 44 (2006) 692.
[33] B.B. Fitts, V.R. Landi, S.K. Roy, US Patent 6,811,917 (2004).
[34] Z. Jie, Z.Y. Wen, H. Jun, J. Zhejiang Univ. Sci. 6A (2005) 1080.
[35] Z. Bin, M. Bingchu, S. Chunhui, Y. Runzhang, J. Power Sources 161 (2006) 997.
[36] Website: http://carbon.myweb.hinet.net/, Great Carbon Co., Ltd.
[37] Website: http://www.fpg.com.tw/html/com/yccic/yccic.html, Yung Chia Chemical Ind., Co., Ltd.
[38] H. Zhang, Z. Zhang, Eur. Polym. J. 43 (2007) 3197.
[39] L. Valentini, J. Biagiotti, J.M. Kenny, S. Santucci, Compos. Sci. Technol. 63 (2003) 1149.
[40] Y. Liu, J.Y. Lee, L. Hong, J. Appl. Polym. Sci. 89 (2003) 2815.
[41] Y.J. Wang, D. Kim, Electrochim. Acta 52 (2007) 3181.
[42] L.G. Xia, A.J. Li, W.Q. Wang, Q. Yin, H. Lin, Y.B. Zhao, J. Power Sources 178 (2008) 363.
[43] L.D. Andrew, J. Power Sources 156 (2006) 128.
[44] E.A. Cho, U.S. Jeon, H.Y. Ha, S.A. Hong, I.H. Oh, J. Power Sources 125 (2004) 178.
[45] T. Ramanathan, F.T. Fisher, R.S. Ruoff, L.C. Brinson, Chem. Mater. 17 (2005) 1290.
[46] Y. Chen, Y. Chen, W. Chen, D. Yang, Eur. Polym. J. 43 (2007) 2999.
[47] P. Doshev, R. Lach, G. Lohse, A. Heuvelsland, W. Grellmann, H.J. Radusch, Polymer 46 (2005) 9411.
[48] S. Chunhui, P. Mu, H. Zhoufa, Y. Runzhang, J. Power Sources 166 (2007) 419.